acta physica slovaca vol. 54 No. 3, 233 – 243 **June 2004**

DYNAMICS OF PHASE CHANGES AND MELTING OF Pd_7 CLUSTERS

M. Karabacak[1†*], **S. Özçelik**[2†], **Ziya B. Güvenç**[3‡]
[†] *Department of Physics, Gazi University, 06500 Teknikokullar, Ankara, Turkey*
[*] *Department of Physics, Afyon Kocatepe University, 03040, Afyon, Turkey*
[‡] *Department of Electronic and Communication Engineering, Çankaya University*
06530, Ankara, Turkey

Received 7 January 2003, accepted 10 March 2004

We have obtained the stable geometrical structures, energetics, melting behaviors and phase changes of Pd_7 clusters by using molecular dynamics and thermal quenching simulations. Cohesion of the clusters is modeled by an embedded-atom potential, which contains many-body atomic interactions. Isomers' energy-spectrum-width and their sampling probabilities are calculated. Melting phenomenon of a cluster is described in terms of relative root-mean-square bond-length fluctuations, and of behavior of the specific heats. The transition region from solid- to liquid-like phases is investigated, and the melting temperature of the cluster is estimated. Minimum energy pathways for the phase changes among the isomers of the Pd_7 are determined.

PACS: 31.15.Qg, 36.40.Ei, 36.40.Qv

1 Introduction

Clusters are finite aggregates with unique physical and chemical properties. Therefore, the structure and dynamics of clusters have been subjects of many theoretical and experimental studies in the last several decades [1-16]. Especially size dependence of the reactivity, structural symmetry, phase and phase-change features of the clusters have been and remained in active research areas of the theoretical studies [1-4]. On the experimental side, chemical reactions have been used as probes of various structural features of the metal clusters [14]. Theoretical calculations can complement such experimental investigations for the properties of interest. These studies, today, have set up a new scientific field so-called "nano-science". Researches have become possible in these areas due to the development of methods and characterization of clusters of various materials. The most important predictions of the theoretical studies are a possible coexistence region of the solid- and liquid-like phases of the clusters over a finite range of energies, drastic changes in the melting temperatures with the size of the systems, and the structure reactivity correlations

---

[1] E-mail address: karabacak@aku.edu.tr
[2] E-mail address: suleyman@gazi.edu.tr
[3] E-mail address: guvenc@cankaya.edu.tr

[15, 16]. In our previous study [1] we discussed the structures, energetics, and isomer formation probabilities of the small Pd clusters. These properties of the clusters play important role for phase changes phenomenon of the clusters.

In the present work, we have focused on the dynamics of phase changes, and melting of four isomers of a Pd_7 cluster. The dynamics of the initially non-rotating and non-translating Pd_7 cluster have been monitored as their internal energies are gradually increased. This size is important since it forms the backbone of the icosahedral symmetry [1]. It has been observed that the Pd_7cluster also exhibit a so-called coexistence stage over a finite range of temperatures before the liquid-like phase, i.e., if one assumes an ensemble of Pd_7 clusters at about 700 K, simultaneously all isomers may exist due to the phase changes between the isomers (see Fig. 6). The melting temperature of the Pd_7cluster is estimated to be ≈ 770 K which is much lower than the bulk melting (1825 K) temperature. The smaller melting temperatures compared to the bulk for small transition metal clusters have also been reported in some other theoretical studies [5, 6, 12, 13, 17, 18] and in a few experimental studies for the large gold clusters [19]. Furthermore, we report the structures and energetics of the stable isomers of the Pd_7, isomers' energy-spectrum-width (ESW), their probability of sampling, and the melting behaviors of these Pd_7 clusters by employing an embedded-atom-method (EAM) potential [20, 21], and constant-energy molecular dynamics (MD) method. The isomeric forms of the Pd_7 cluster were determined by thermal quenching (TQ) technique. Possible minimum energy pathways for the phase changes among the isomers of the Pd_7 cluster are determined. The details of the potential energy surface and computational procedure are given in the next Section. In Section 3 the results are discussed, and we conclude with a summary.

2 Potential and computational procedure

The total potential energy surface defining the forces acting on each atom in the cluster system is an N-body EAM. The cohesion energy of a metallic system is obtained by the sum of all the interaction energies in N-atom system, and it is expressed as

$$V = \sum_i \left[F_i(\bar{\rho}_i) + \frac{1}{2} \sum_{j(\neq i)} \phi_{ij}(r_{ij}) \right], \tag{1}$$

where $F_i(\bar{\rho}_i)$ is the so-called embedding energy of atom i in the host of the other atoms, $\phi_{ij}(r_{ij})$ is the core-core pair interaction between atoms i and j, and r_{ij} is the distance between atom i and j. The host electron density $\bar{\rho_i}$ is approximated by a linear superposition of all the atoms surrounding atom i,

$$\bar{\rho}_i = \sum_{j(\neq i)} \rho(r_{ij}), \tag{2}$$

$$\rho(r_{ij}) = r_{ij}^6 (e^{-\beta r_{ij}} + 2^9 e^{-2\beta r_{ij}}), \tag{3}$$

where $\bar{\rho}(r_{ij})$ is the electron density (for Pd, $\beta = 3.1632$ Å^{-1}) created by atom j at the position of atom i [21].

The melting behavior of the clusters was investigated by the root-mean-square (RMS) bond-length fluctuation δ,

$$\delta = \frac{2}{N(N-1)} \sum_{i<j} \frac{(\langle r_{ij}^2 \rangle - \langle r_{ij} \rangle^2)^{1/2}}{\langle r_{ij} \rangle} \tag{4}$$

calculated at different total energies. Here, $\langle \cdot \rangle$ denotes the long-time average calculated over the entire trajectory (over 5×10^6 time steps) for a given total energy. Initially the non-rotating and non-translating cluster's internal energy has been increased stepwise manner, and the vibrational kinetic energy is scaled as

$$T(K) = \frac{2\langle E_k \rangle}{(3N-6)k} \tag{5}$$

to obtain the temperature $T(K)$. Here E_k is the internal kinetic energy of the cluster, k is the Boltzmann constant, N is the number of atoms in the cluster, and (3N – 6) is the internal degrees of freedom of the system. The stable geometrical structures of a Pd_7 cluster are identified using MD and TQ simulations [1]. Evolution of the N-atom system in the phase-space has been monitored using Hamilton's equations of motion with Hamming's modified 4^{th} order-predictor-corrector algorithm with a step-size of 1×10^{-15} s. The cluster is equilibrated at near 2500 K for about 5 ns before the calculation of any physical quantities. After the equilibration, a large number of independent initial quenching configurations (sample size of 5000) are generated along a new trajectory at the same temperature (these configurations are 1000 simulation steps apart from each other). These independent initial configurations are used to calculate isomer-statistics. Since the internal energies are much higher than the melting temperature, 1000-step separation between the configurations is adequate to generate different phase-space points. The TQ technique is used to remove the internal kinetic energy of the clusters; the internal kinetic energy is set to zero at every 50^{th} step, and this process has continued until the kinetic energy is completely removed. Because of this slow minimization process, clusters cannot stay at meta-stable locations of the potential energy surface, and finally, they will settle in the potential energy "wells". Thus, the locally stable isomers are separated from those meta-stable ones. As a result we have obtained four different stable isomers of the Pd_7 (see Fig. 1), and their probabilities of sampling are computed. The structures, energetics, melting behaviors of these four isomeric forms and the ESW (energy difference between energetically the lowest and the highest isomers) of the cluster are discussed in the next Section.

3 Results and Discussion

In addition to the energetics and geometries (see Fig. 1) of the stable isomers of the Pd_7 cluster [1], their averaged bond lengths and phase changes are also calculated. We have found that the most stable geometrical structure of the Pd_7 cluster is a pentagonal bipyramid, and obtained three other stable isomers. The second lowest energy structure is a capped octahedron, which can be obtained from the lowest energy structure of the Pd_6 (octahedron) by simply capping one of the faces of the Pd_6. The energy difference between these two structures (the 1^{st} and the 2^{nd} isomers) is 0.28 eV. When a free Pd atom lands on the surface of the Pd_6 cluster which are both at room temperature, the Pd_7 cluster is formed (Pd_6 + Pd $\rightarrow Pd_7$). Exothermicity of this reaction

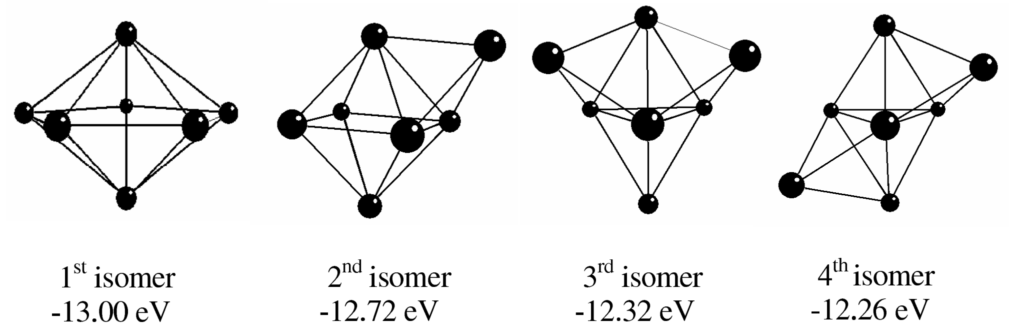

Fig. 1. Isomers of the Pd_7 cluster.

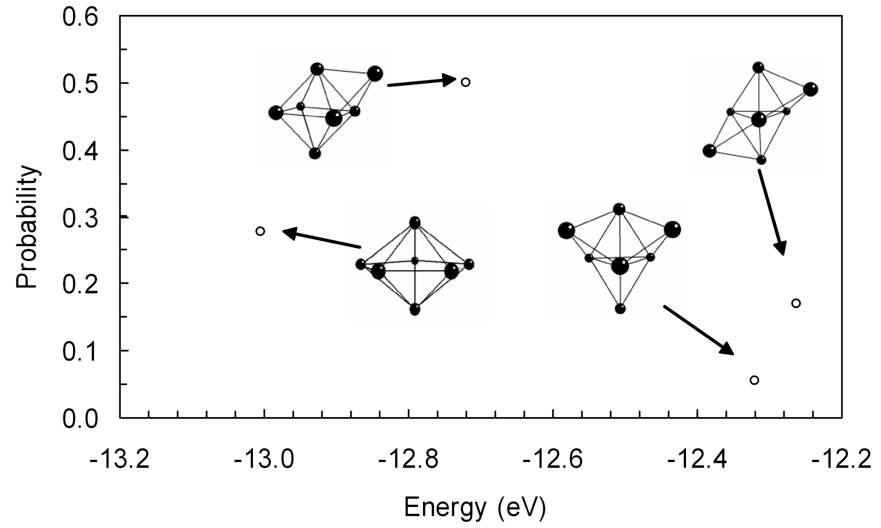

Fig. 2. This Figure is taken from Figure 2 of Ref. [1]. Isomer-forming probabilities of the Pd_7cluster. Each point in the graph corresponds to a different isomer of the cluster and corresponding energies are the energies of the quenched isomers.

melts the cluster, and in vacuum the cluster will remain as melted. However in the experiment, while the small clusters are "melting" as they form, the He carrier gas has continuously cooled them down simultaneously. The energetics of the process is given as follow; the total energy of the Pd_6 cluster at 300 K is near -9.96 eV, and the total energy of the second isomer of the Pd_7 is about -12.32 eV at 300 K. The difference is 2.36 eV which is being dissipated to the surrounding, i.e., to the carrier gas. On the other hand, the Pd_7 cluster melts at the total energy of -11.9 eV which is less than the energetics of the Pd_6 at 300 K. This shows that in the experiment the small clusters melt as they form. Therefore the memory of the growth path is lost. In this sense, our TQ simulation is somewhat similar to the cooling process of the hot molten cluster in the experiment. As seen from the TQ simulation, half of the molten clusters are quenched into the capped octahedron structure, which may also be the case in the experiment. In the other half, the 1^{st}, the 3^{rd}, and the 4^{th} isomers are distributed with 0.27, 0.05, and 0.18 probabilities, respectively. These isomer-forming probabilities are calculated from the 5000 phase-space points, and they are displayed in Fig. 2. The second isomer may have a wider potential well and there are eight identical states in the phase-space for it. These facts determine the isomer-forming probabilities. The other two isomers are topologically and energetically close to each other (both of them are capped trigonal bipyramid and the energy difference between them is about 0.06 eV). The two surface atoms, for the third isomer, are on the adjacent faces of the same polar region. Similarly, the fourth isomer has also two surface atoms however they are on the opposite faces (maximum distance is formed between the capping atoms). Therefore, there are six identical states (topology) for the third, and the fourth isomers. However, the isomer-forming probability is higher for the 4^{th} one compared to that of the 3^{rd} one. Since the energy difference between the 4^{th} and the 3^{rd} isomers is small and the numbers of accessible states are the same, in this case, the shape and the width of the potential energy well may play role. The isomer-forming probability, $P_n(E)$, in general may be proportional with $\exp(c/(E_n + |E_h|)$, here E_n is the energy of the n^{th} isomer ($E_n < 0$), E_h is the energy of the last isomer (in this case it is the 4^{th} isomer), and c is a size dependent constant in units of eV (i.e., higher the energy, lower the isomer-forming probability). It is observed that at temperatures $\approx$ 300 K the 1^{st} and the 2^{nd} isomeric forms can be seen via phase changes (Fig. 6(b)). Therefore, both isomers may coexist under the experimental condition near room temperature. If the reactivities of these isomers with small molecules are sufficiently different, then, they can be distinguished in the experiment. Further, the ESW of the isomers is computed as 0.74 eV. In addition, the average bond lengths, $\langle d \rangle$, of the quenched four isomers of the Pd_7 cluster, from the first to the fourth, are calculated as 2.554 Å, 2.536 Å, 2.551 Å, and 2.547 Å, respectively, where the bulk value is 2.75 Å.

The earlier theoretical studies used the effective medium potential in Ref. [11], the EAM model potential [12,13], and modified semi-empirical extended Hünkel (EH) calculation [22] have predicted that the preferred structure for the Pd_7 is a pentagonal bipyramid. However, there are some energy differences among these studies. Stave et al. [11], using the corrected-effective-medium (CEM) and MD / MC - CEM theories, obtained that the binding energies of the pentagonal bipyramid are –13.94 and –12.90 eV, respectively. Rey et al. [13] computed this energy as about –20 eV using a tight-binding and the original version of the EAM [20] methods. We have obtained –13.00 eV for the binding energy of the pentagonal bipyramid. Furthermore, they also obtained three energetically different isomers. Our third and the fourth isomers are energetically closer to each other compared to those of Refs. [11,13]. Quantum chemical study of small palladium clusters was reported by Efremenko et al. [22]. The pentagonal bipyramid

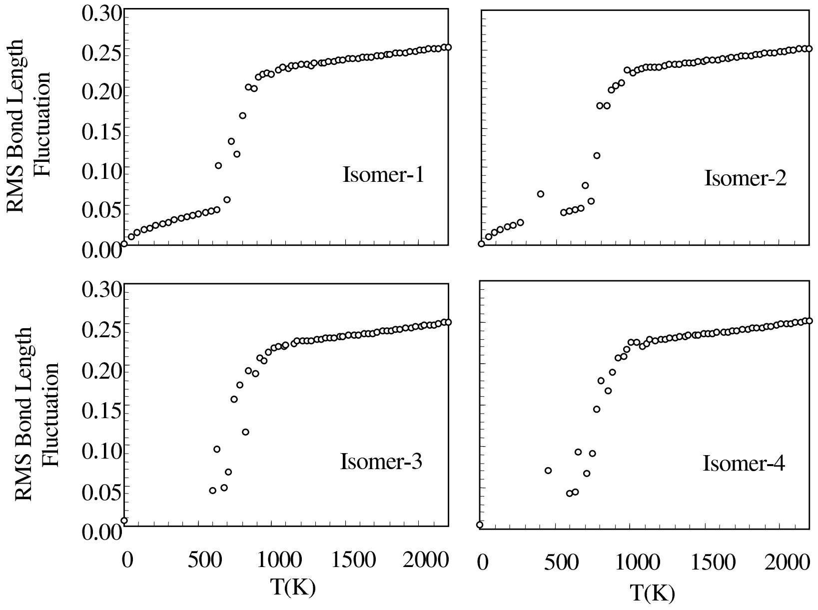

Fig. 3. RMS bond-length fluctuations versus temperature of the isomers.

form has -11.44 eV (highest occupied molecular orbital) energy level. Further, the bond distances are reported as 2.56 Å and 2.63 Å for the same structure in Ref. [22]. These distances correspond to the distance between the two adjacent atoms in the pentagonal ring, and from any atom in the ring to the one of the capping atoms, respectively. Our calculated distances for the same cases are 2.52 Å and 2.55 Å, respectively. These show that our results are in reasonable agreement with those of Ref. [22]. In addition, our model potential energy is also checked against to the local density functional approach [23] by comparing the averaged bond lengths of the smaller sizes of the Pd clusters; Pd_4, Pd_6 and Pd_8. The averaged bond lengths (calculated in our work using the EAM) of these clusters are 2.533 Å, 2.529 Å, and 2.531 Å, respectively. They are reported as (in Ref. [23]) 2.661 Å, 2.718 Å, and 2.661 Å using GGA, and 2.591 Å, 2.634 Å, and 2.571 Å using LDA, respectively. As seen, there are small differences, and a similar trend between the Pd_4, Pd_6, and Pd_8 clusters are not reproduced by these three methods.

In order to understand the melting mechanisms of the isomers the RMS bond-length fluctuations are plotted as a function of the internal kinetic energy (temperature), (see Fig. 3), and average kinetic energies are plotted as a function of the total energy (see Fig. 4). As shown in Fig. 3, the melting behavior of the first isomer is similar to those of Lennard-Jones clusters [24, 25]: when the internal energy is increased, the cluster changes its form from a solid-like to a liquid-like phase via an intermediate stage (transition region). The transition region from the solid- to liquid-like states is spread over 300 K (approximately from 600 K to 900 K). The temperature corresponds to the middle point of the sharply increased region ($\delta \cong 0.18$) is taken as the melting temperature of the cluster (with an estimated uncertainty of about ± 5 %). As seen from Fig. 3 the most stable isomer's melting temperature is at about 770 K. The bulk melting

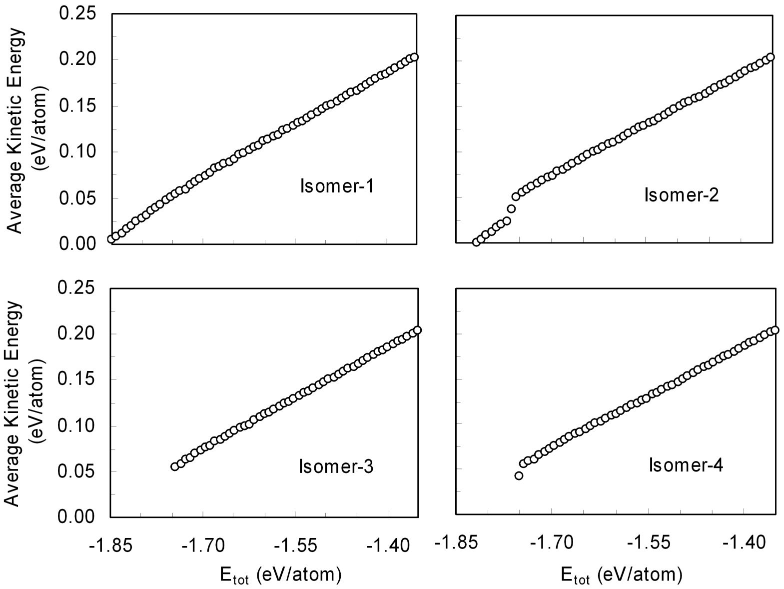

Fig. 4. Average kinetic energy per atom versus total energy per atom for the four isomers.

temperature (1825 K) is much higher than the melting temperature of the Pd_7 [26]. The other isomers are converted to the most stable isomer before they melt. Therefore, all isomers follow a similar melting "path". As a result, the Pd_7 cluster has only one melting temperature (770 K). The second isomer is converted into the first isomer near 300 K. However, transformations of the third and the fourth isomers begin at very low temperatures (near 50 K and 4 K, respectively). This shows that potential energy "wells" of the 3rd and the 4th isomers are quite shallow. Furthermore, the 3rd and 4th isomers do not show classical melting transitions. Instead, these isomers move into the transition region quickly from their minimum energy configurations. Because of 0.68 eV difference in the potential energies between the 1st and the 3rdisomers, half of this energy goes into the internal kinetic energy as cluster changes its structure, the 3rd isomer moves quickly to the beginning of the melting state (origin of the discontinuity in the RMS value, and its high temperature is due to this energy difference). The melting behavior of the 4th isomer is very similar to that of the 3rdone as seen in Fig. 3. One can also see from Fig. 4 (caloric curves) that pentagonal bipyramid structure at about -1.73 eV/atom has begun isomerisation transition (slope of the curve changes near this energy). If the internal energy is increased further, the cluster is converted into liquid-like form. The transformation of the capped octahedron (2nd isomer) to the pentagonal bipyramid form at -1.77 eV/atom leads to a sudden increase in the internal kinetic energy (see Figs. 3 and 4). Similarly, transformations of the 3rd and 4th isomers also create discontinuity in the caloric curves (Fig. 4).

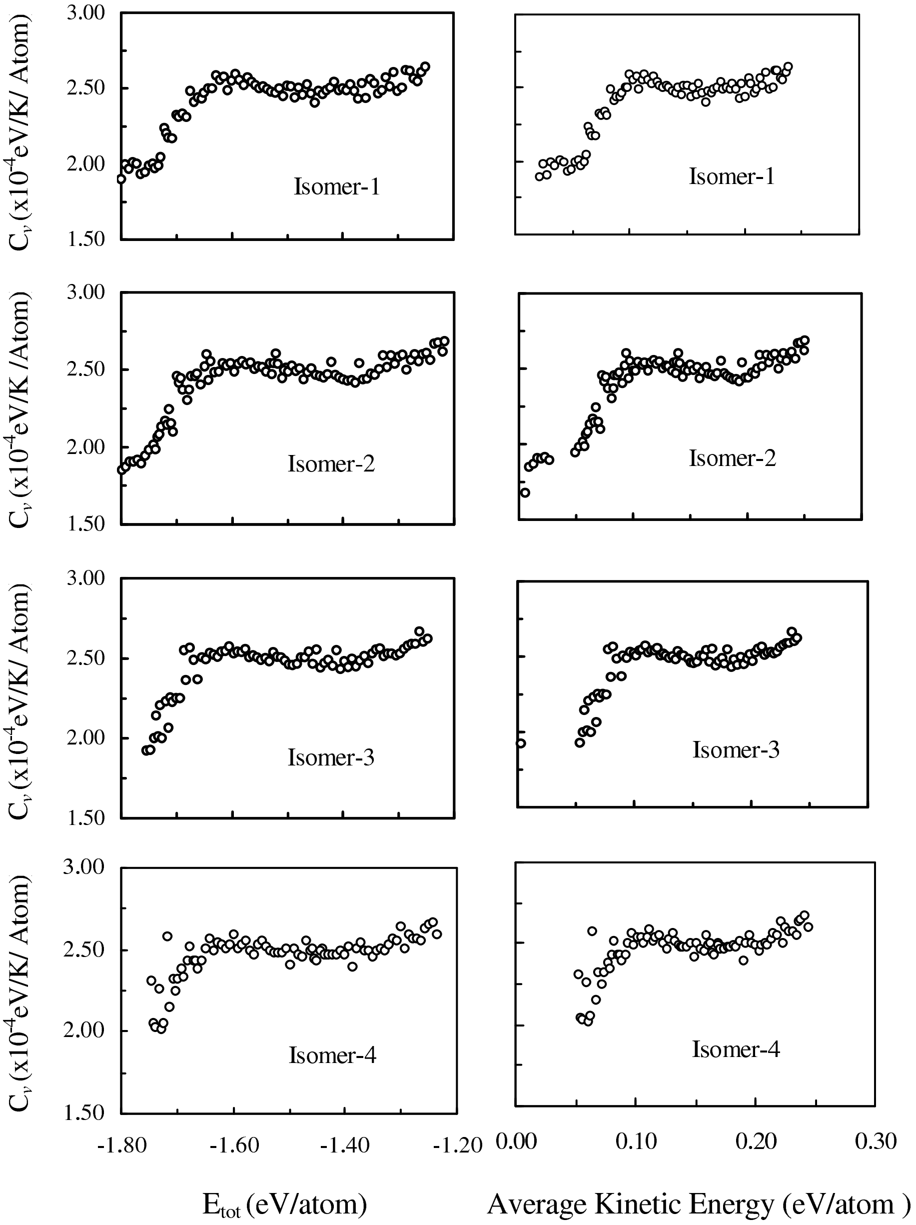

Fig. 5. Specific heat per atom (C_v) for the four isomers of the Pd_7 cluster as functions of the total and average kinetic energies in unit of eV/atom.

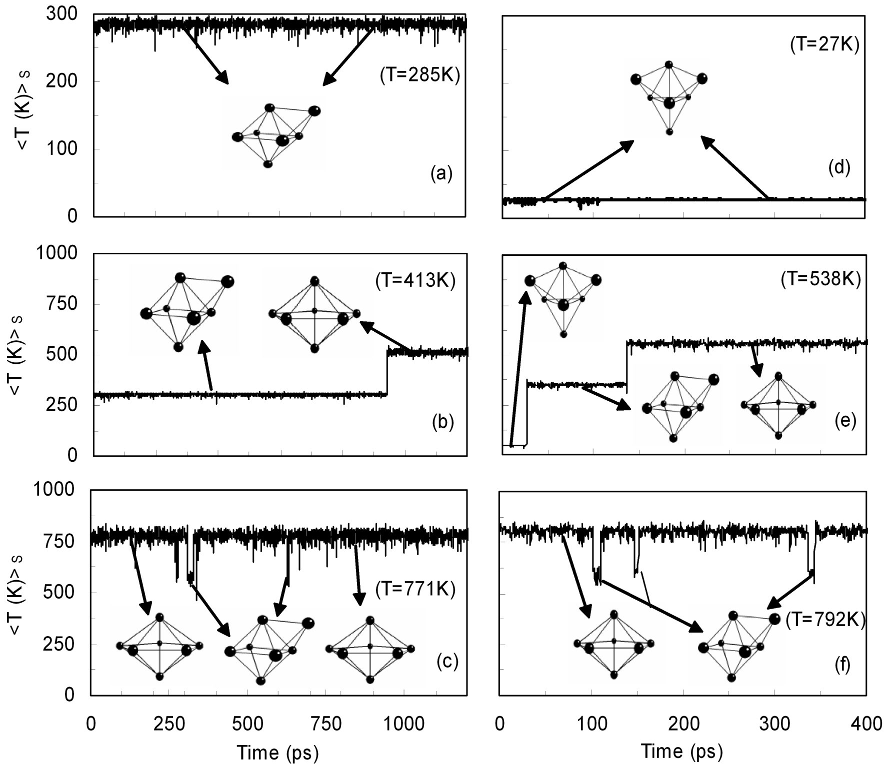

Fig. 6. Short time average of the temperatures, $\langle T(K)\rangle$s, for the 2^{nd} (from (a) to (c)) and for the 3^{rd} (from (d) to (f)) isomers of the Pd$_7$ cluster as a function of time (ps). Internal energies of the isomers are increasing from (a) to (c), and from (d) to (c). The temperatures in the figures are the averaged temperatures over the entire trajectory.

Specific heats per atom [27] is calculated from

$$C_v = \left[n - n\left(1 - \frac{2}{3n-6}\right)\langle E_k\rangle\langle E_k^{-1}\rangle\right]^{-1} \tag{6}$$

for the four isomers of the Pd$_7$ as functions of the total energy per atom and average kinetic energy per atom, and they are given in Fig. 5. The energy values of the specific heats where the slops of the curves change rapidly on the left hand side of the peaks correspond to the beginning of the melting of these isomers. As seen, the beginning of the phase changes and the liquid-like state is in between -1.74 eV/atom and -1.62 eV/atom, as the total energy (or from 0.057 eV/atom to 0.100 eV/atom as the average kinetic energy). This region also corresponds to 670 K – 950 K. Behaviors of the other isomers are very similar to that of the 1^{st} isomer since they are eventually converted into the form of the 1^{st} one before they begin to melt.

In order to understand the dynamics and the order of the phase changes of the 2^{nd}, the 3^{rd}, and the 4^{th} isomers, the short-time averaged (averaged over 1250 time steps) temperatures, $\langle T(K)\rangle$s,

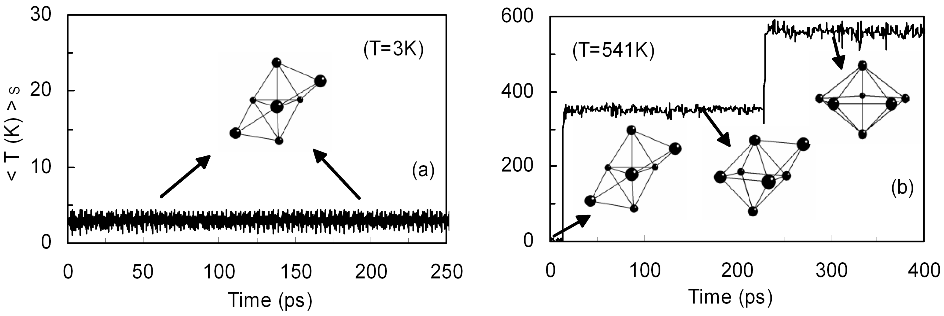

Fig. 7. The same as Fig. 6 for the 4^{th} isomer.

are displayed as a function of the simulation time in Figs. 6 and 7. As seen, the 2^{nd} isomer (Figs. 6(a) – 6(c)) near room temperature is transformed into the 1^{st} one (Fig. 6(b)). As the temperature increases, the phase change from the $1^{\text{st}} \Leftrightarrow 2^{\text{nd}}$ one is more frequent (Fig. 6(c)). At higher internal energies (near melting) $3^{\text{rd}} \Leftrightarrow 2^{\text{nd}} \Leftrightarrow 1^{\text{st}}$ transitions take place. Eventually the 4^{th} isomer is seen (not shown), and the fluctuations in the kinetic energies are much larger. The 3^{rd} isomer (Figs. 6(d) and 6(f)) goes through $3^{\text{rd}} \longrightarrow 2^{\text{nd}}$ at very low temperature (≈ 50 K). After this point, dynamics of the phase changes and the order of the transitions are very similar to that of the 2^{nd} isomer discussed above, i.e., from $2^{\text{nd}} \longrightarrow 1^{\text{st}}$ is seen near room temperature. If one starts with the 4^{th} isomer (see Fig. 7), then, the transition from the 4^{th} to the 2^{nd} isomer takes place first at about 4 K. This shows that the potential energy well depth is very shallow. The orders: $2^{\text{nd}} \longrightarrow 1^{\text{st}}$, $3^{\text{rd}} \longrightarrow 2^{\text{nd}}$, and $4^{\text{th}} \longrightarrow 2^{\text{nd}}$ are the possible minimum energy pathways for the phase changes. This can be understood from Fig. 1. Finally, in order to check the isomer spectrum as a function of temperature similar runs were made above 2500 K. However, before all the initial conditions are formed, fragmentation of the Pd_7 cluster is observed. Therefore, we believe that these four stable isomers of the cluster form the spectrum. In our simulation, too shallow/narrow potential wells cannot be found due to the numerical errors.

4 Summary

Size 7 for the Pd cluster is important since it forms the backbone of the icosahedral structure. Therefore, in this work, the number of stable isomers, their energetics, structures, melting behaviors, isomer-forming probabilities of the Pd_7 cluster, and the phase changes are discussed. The isomer-forming probabilities depend on the isomer's energy, symmetry, number of accessible states for a given energy, and the shape and the width of the potential energy well. The melting behavior is characterized by the RMS bond-length-fluctuation. The first isomer shows similar melting behavior to those of Lennard-Jones clusters. On the other hand caloric curves and the RMS values of the other isomers (energetically higher) have discontinuity because of the phase changes from higher isomeric forms to the lower isomeric forms. Discontinuities in the caloric curves and the RMS depend on the energy difference between these isomers and the 1^{st} one.

Specific heat graphs display peaks for all the isomers nearly at the same total energy values. All these show that melting temperatures for the Pd_7 is about 770 K. Short-time averaged temperature versus time figures clearly displays the phase changes between the isomers. The orders of the phase changes which require least energies are $2^{\mathrm{nd}} \rightarrow 1^{\mathrm{st}}$, $3^{\mathrm{rd}} \rightarrow 2^{\mathrm{nd}}$, and $4^{\mathrm{th}} \rightarrow 2^{\mathrm{nd}}$.

Acknowledgement: This work at Gazi University was supported by Turkish Republic of Prime Ministry State Planning Organization (Procet Number: 2001K120590).

References

[1] M. Karabacak, S. Özçelik, Z.B. Güvenç: *Surf. Sci.* **507** (2002) 636; and references therein.
[2] E.R. Bernstein: *Atomic and Molecular Clusters*, Elsevier, Amsterdam 1990
[3] G. Benedek, M. Pacchioni: *Elemental and Molecular Clusters*, Springer, Berlin 1988
[4] J. Jellinek (Eds.): *Theory of atomic and molecular clusters*, Springer, Berlin 1999
[5] Z.B. Güvenç, J. Jellinek, A.F. Voter: *Physics and Chemistry of Finite Systems: From Clusters to Crystals*, (Eds. P. Jena, S.N. Khanna, B.K. Rao). **I** 411, Kluwer Academic, Dordrecht 1992
[6] Z.B. Güvenç, J. Jellinek: *Z. Phys. D* **26** (1993) 304
[7] E. Curotto, A. Matro, D.L. Freeman, J.D. Doll: *J. Chem. Phys.* **108** (1998) 729
[8] Z.B. Güvenç, D. Güvenç, J. Jellinek: *Int. J. Mathematical & Computational Applications* **4** (1999) 75
[9] S. Sugano, Y. Nishini, S. Ohnisni: *Microclusters*, Springer, Berlin 1987
[10] E.R. Bernstein: *Atomic and Molecular Clusters*, Elsevier, Amsterdam 1990
[11] M.S. Stave, A.E. DePristo: *J. Chem. Phys.* **97** (1982) 3386
[12] J. Garcia-Rodeja, C. Rey, L.J. Gallego, J.A. Alonso: *Phys. Rev. B* **49** (1994) 8495
[13] C. Rey, L.J. Gallego, J. Garcia-Rodeja, J.A. Alonso, M.P. Iniguez: *Phys. Rev. B* **48** (1993) 8253
[14] E.K. Parks, L. Zhu, J. Ho, S.J. Riley: *J. Chem. Phys.* **100** (1994) 7206
[15] J. Jellinek, Z.B. Güvenç: *Z. Phys. D* **26** (1993) 110
[16] J. Jellinek, Z.B. Güvenç: *in The Synergy Between Dynamics and Reactivity at Clusters and Surfaces*, (Eds. L.J. Farrugia). Kluwer, Dordrecht 1995, p. 217
[17] J. Jellinek, I.L. Garzon: *Z. Phys. D* **20** (1991) 239 ; I.L. Garzon, J. Jellinek: *Z. Phys. D* **20** (1991) 235 ; H.-P. Cheng, R.S. Berry: *Phys. Rev. A* **45** (1992) 7969
[18] S. Sawada, S. Sugano: *Z. Phys. D* **14** (1989) 247
[19] Ph. Buffat, J.P. Borel: *Phys. Rev. A* **13** (1976) 2287 ; J.P. Borel: *Surf. Sci.* **106** (1981) 1
[20] M.S. Foiles, M.I. Baskes, M.S. Daw: *Phys. Rev. B* **33** (1986) 7983
[21] A.F. Voter: *Los Alamos Unclassified Technical report* # LA-UR 93-3901 1993
[22] I. Efremenko, M. Sheintuch: *Surface Science* **411** (1998) 148
[23] S. Krüger, S. Vent, F. Nörtemann, M. Staufer, N. Rösch: *J. Chem. Phys.* **115** (2001) 2082
[24] T.L. Beck, J. Jellinek, R.S. Berry: *J. Chem. Phys.* **87** (1987) 545
[25] I.L. Garzon, M. Avalos-Borja, E. Blaisten-Barojas: *Phys. Rev. B* **40** (1989) 4749
[26] R. Hultgren, P.D. Desai, D.T. Hawkins, M. Gleiser, K.K. Kelley, D.D. Wagman: *Selected Values of the Thermodynamic Properties of the Elements*, American Society for Metals, Metals Park, Ohio 1973
[27] E.M. Pearson, T. Haliciolu, W.A. Tiller: *Phys. Rev. A* **32** (1985) 3030